Available online at www.sciencedirect.com
SCIENCE DIRECT®
Journal of Molecular Catalysis A: Chemical 228 (2005) 275–282
JOURNAL OF MOLECULAR CATALYSIS A: CHEMICAL
www.elsevier.com/locate/molcata

Improved sulfur resistance of Pt-Sn/γ-Al_2O_3 catalysts for C_3H_8-NO-O_2 reaction under lean conditions due to Pt-Sn surface interactions

Grisel Corro[a,*], J.L.G. Fierro[b], Ramón Montiel[a], Fortino Bañuelos[a]

[a] *Instituto de Ciencias, Benemérita Universidad Autónoma de Puebla, 14 Sur 6301, Puebla 72570, Mexico*
[b] *Instituto de Catálisis y Petroleoquímica, CSIC, Cantoblanco, 28049 Madrid, Spain*

Available online 11 November 2004

Abstract

The selective catalytic reduction (SCR) of NO with C_3H_8 was studied over unsulfated and pre-sulfated 1% Pt/γ-Al_2O_3, and 1% Pt-2% Sn/γ-Al_2O_3 catalysts. Carbon residues deposited were evaluated on all samples, after 12 h of C_3H_8-NO-O_2-SO_2 reaction. X-ray photoelectron spectra (XPS) were recorded over unsulfated and pre-sulfated fresh samples. Pre-sulfated 1% Pt-2% Sn/γ-Al_2O_3 catalyst showed a high resistance to deactivation by sulfur during C_3H_8-NO-O_2-SO_2 reactions. Results are explained on basis of the effect of tin addition to 1% Pt/γ-Al_2O_3 that results in (i) lowering the sulfates generated over the surface of the catalyst during sulfation; and (ii) preventing Pt particles from sintering during sulfation process. We also investigated the effect of Sn addition to 1% Pt/γ-Al_2O_3 catalyst, and the effect of pre-sulfation on 1% Pt/γ-Al_2O_3 and 1% Pt-2% Sn/γ-Al_2O_3, on carbon depositions over the catalysts. Results showed a strong diminution of carbon depositions on sulfated 1% Pt-2% Sn/γ-Al_2O_3 due to Pt-Sn surface interactions. The facts that tin addition to a Pt/γ-Al_2O_3 catalyst, prevents Pt particles from sintering during high temperature sulfation and that sulfating a 1% Pt-2% Sn/γ-Al_2O_3 catalyst prevents carbon residues deposition over the catalyst, suggest that this catalyst could resist high temperature reactions during automotive exhaust control without deactivation.

Keywords: Pt-Sn catalysts; Sulfur deactivation; Lean-burn conditions; NO_x reduction; Particulate emissions

1. Introduction

The selective catalytic reduction of NO_x by hydrocarbons (HC-SCR) has attracted considerable interest as a method to control emissions from engines operated under oxygen-rich conditions. Sulfur amounts in fuel, however, usually play a detrimental role in the performance of HC-SCR catalysts. The sulfur problem is most serious in the catalytic after-treatment of exhaust from diesel engines. At present, the development of a sulfur-resistant HC-SCR catalyst at low temperature may be regarded as a major challenge in catalytic research of diesel engine pollution control. In a similar manner, the large amounts of sulfur present in diesel fuel impede the application of particulate matter filter technologies in which a NO_x catalyst-assisted process is used to facilitate filter regeneration [1]. Despite the continuous efforts to remove sulfur from the fuels, the inlet gas stream in deNO_x units contains sulfur in the form of SO_2. The activity of a catalyst in the presence of SO_2 is decisive for its implementation in practical problems. Parvulescu et al. [2] reviewed the catalytic removal of NO from the flue gases. They acknowledged that the SCR by hydrocarbons is the most promising method to reduce the NO emissions, and classified the catalysts for the SCR by hydrocarbons in three categories: (i) metal-ion exchanged zeolites; (ii) supported noble metals; and (iii) base metal oxides. Platinum and platinum–tin impregnated on alumina belong to type (ii) category.

Noble metals are tolerant to the SO_2 presence in the feed [3,4], while transition metals [3] and particularly silver [5] are deactivated by SO_2 as a result of sulfates formation. Among the various oxide supported noble metal catalysts, Pt/Al_2O_3 has received much attention with regard to its durability in the presence of SO_2 [6–9]. In a study by Burch and Walt-

* Corresponding author. Fax: +52 222 229 5551.
E-mail address: cs001380@siu.buap.mx (G. Corro).

1381-1169/$ – see front matter © 2004 Elsevier B.V. All rights reserved.
doi:10.1016/j.molcata.2004.09.056

ing [9] ex situ sulfated catalysts were demonstrated to be active in NO reduction with propene in the presence of excess oxygen but to loose activity in the same reaction when replacing propene by propane under identical reaction conditions. The difference in the reducing power of propene versus propane was attributed to differences in the reaction mechanisms. In our previous studies [10], we showed the effect of tin addition to Pt-/γ-Al_2O_3 on the $SO_2 + O_2$ reaction. Results demonstrated a lower activity in SO_2 oxidation over Pt-Sn/γ-Al_2O_3 relative to Pt/γ-Al_2O_3. The lowering in SO_2 oxidation resulted in a diminution of sulfates generated over the surface of the catalyst. This fact led us think that Pt-Sn/Al_2O_3 could be resistant to SO_2 deactivation during the selective catalytic reduction of NO_x by hydrocarbons. In the present work, we investigated in detail the activity of Pt/γ-Al_2O_3 and Pt-Sn/γ-Al_2O_3 (both unsulfated and pre-sulfated) on C_3H_8-NO-O_2 reaction. We will explain the catalytic behavior of the catalysts on basis of the Pt-Sn surface interactions determined by XPS.

Now, alumina-supported Pt-Sn catalysts have been the subject of many studies because of the importance of these catalysts in refining and petroleum chemistry, particularly in reforming reactions [11–15]. In general, it has been accepted that Sn addition to Pt increases the stability of the catalyst, increasing its resistance to deactivation by carbonaceous residues deposition. This means that Pt-Sn/γ-Al_2O_3 could prevent this deposition of carbonaceous species that may contribute to further particulate formation over the catalyst during automotive exhaust control. Thus, in this work, we also investigated:

- Carbon residues deposited on Pt/γ-Al_2O_3 and Pt-Sn/γ-Al_2O_3, after 12 h of C_3H_8-NO-O_2 reaction, to elucidate the influence of tin and how possible alloying influences carbon deposition over a Pt/γ-Al_2O_3 catalyst.
- Carbon residues deposited on Pt/γ-Al_2O_3 and Pt-Sn/γ-Al_2O_3 both pre-sulfated, after 12 h of C_3H_8-NO-O_2-SO_2 reaction, to determine the effect of sulfates formation over Pt/γ-Al_2O_3 and Pt-Sn/γ-Al_2O_3 on the carbon residues deposition.

2. Experimental

The support used was γ-Al_2O_3 Merck with a grain size of 0.063–0.200 mm (70–230 mesh ASTM). Before use, the support was calcined for 6 h at 600 °C in air. Pt and Pt-Sn catalysts supported on alumina were prepared by impregnation using acidic aqueous solutions (0.1 M HCl) of $SnCl_4 \cdot 5H_2O$ (Alfa/Johnson Matthey) and $H_2PtCl_6 \cdot 6H_2O$ (Merck, min. 98% purity). After impregnation, the catalysts were dried at 120 °C overnight, and then calcined in flowing air for 6 h at 500 °C. Finally, the catalysts were reduced in pure hydrogen flow for 8 h at 500 °C. A reference alumina support was prepared in the same way using only diluted hydrochloric acid. A sample of the reduced catalysts was then sulfated. Sulfation was performed on samples heating to 500 °C in flowing air (100 $cm^3\ min^{-1}$). The feed was then changed at 500 °C for a nitrogen flow containing 50 ppm of SO_2, 5% O_2 (100 $cm^3\ min^{-1}$) for 10 h. The samples were then cooled to 25 °C.

Platinum accessibility measurements on reduced catalysts, were obtained by the H_2–O_2 titration method at room temperature in a static volumetric apparatus and using the stoichiometric $(H/Pt)_{surf} = 1$. Isotherms were obtained in the 0–50 Torr (1 Torr = 1.33 mbar) range. Extrapolation of the linear part of the isotherm to zero pressure gave the monolayer coverage. This amount of H_2 chemisorbed in monolayer was then used to calculate the number of exposed Pt atoms and dispersion (Table 1). Comparable Pt dispersion values were obtained for the mono and the bimetallic catalysts, respectively.

The chemical microanalysis of the catalyst was determined by energy dispersive X-ray spectroscopy (EDS), (NORAN) performed in conjunction with a scanning electron microscope (JEOL, model JSM-6300). Chemical microanalysis determinations are reported in Table 1.

Photoelectron spectra were recorded over unsulfated and pre-sulfated fresh samples using a VG Escalab 200R spectrometer equipped with a hemispherical analyzer, operating in a constant pass energy mode, and a non-monochromatic Mg Kα ($h\nu = 1253.6$ eV, $1\ eV = 1.603 \times 10^{-19}$ J) X-ray source operated at 10 mA and 12 kV. The energy regions of the photoelectrons of interest were scanned a number of times in order to get good signal-to-noise ratios. The intensities of the peaks were estimated by determining the integral of each peak after subtracting an S-shaped background and fitting the experimental peak to Lorentzian/Gaussian lines (80% L/20% G). The binding energies (BE) were referenced to the Al 2p peak, the BE of which was fixed at 74.5 eV. Using this reference, BE values of C 1s peak coming from adventitious carbon appeared at 284.9 ± 0.2 eV.

The catalytic tests were performed in a continuous flow tubular quartz reactor (inner diameter 7 mm) placed in a

Table 1
Chemical microanalysis of the catalysts determined by energy dispersive X-ray spectroscopy and Pt dispersion determined by H_2 chemisorption data

Catalyst	wt.% Pt	wt.% Sn	wt.% Cl	wt.% S	Pt dispersion
γ-Al_2O_3	–	–	0.99	2.4	–
1% Pt/γ-Al_2O_3	1.02	–	1.2	–	0.35
1% Pt/γ-Al_2O_3 pre-sulfated	1.02	–	1.0	1.8	–
1% Pt-2% Sn/γ-Al_2O_3	1.0	2.2	1.2	–	0.28
1% Pt-2% Sn/γ-Al_2O_3 pre-sulfated	1.0	2.2	1.1	1.4	–

programmable furnace. The catalyst temperature was controlled by a thermocouple mounted internally. Reactant gases were fed from independent mass flow controllers. Measurements over unsulfated samples were performed using a feed volume flow rate of 100 $cm^3\,min^{-1}$ consisting of 1000 ppm of NO, 2.5 vol.% of C_3H_8, 15 vol.% of O_2, and balance He. The catalyst loading in the reactor was of 200 mg. Sulfated samples (200 mg) were exposed to a gas flow consisting of 1000 ppm of NO, 2.5 vol.% of C_3H_8, 50 ppm of SO_2, 15 vol.% of O_2, and balance He to yield a total flow of 100 $cm^3\,min^{-1}$. The reactor out flow was analyzed using a Shimadzu gas chromatograph provided with a thermal-conductivity detector (TCD). The chromatograph used a Chromosorb 2000 column to analyze the C_3H_8 evolutions and a molecular sieve 13X column for the separation of O_2 and N_2. Measurements were made as the samples were heated in the range 25–500 °C in steps of 50 °C. The catalyst was left at each temperature for 1 h until the steady state was reached. The NO and SO_2 evolutions were followed using a KM 9106 Quintox Gas Analyzer. NO_2 and N_2O yields were determined by a FTIR spectrometer. All samples were left at 500 °C under the reaction flow for 12 h. The sample was then purged at the same temperature in a He flow for 30 min and the temperature then lowered to 25 °C prior to the temperature-programmed oxidation in an air flow of 100 $cm^3\,min^{-1}$. Temperature was ramped at 10 °C min^{-1} while the CO_2 generated was monitored by gas chromatography using a Chromosorb 2000 column.

The conversions of C_3H_8 or SO_2 or NO to all products were calculated based on the following equation:

$$\text{conversion}\,(\%) = \frac{X_{\text{in}} - X_{\text{out}}}{X_{\text{in}}} 100$$

X_{in} is the concentration of X introduced in the experiment; X_{out} the concentration of X at the reactor outlet.

3. Results

3.1. Catalysts characterization

The catalyst characterization data are summarized in Table 1. Comparable Pt dispersion values of 0.35, and 0.28 were obtained for the mono and the bimetallic catalysts, respectively.

3.2. C_3H_8-NO-O_2 reactions over pre-sulfated and unsulfated γ-Al_2O

The effect of temperature on the C_3H_8-NO-O_2 reaction over pre-sulfated and unsulfated γ-Al_2O is shown in Fig. 1. In this figure, it can be seen that in the temperature range studied, pre-sulfated and unsulfated γ-Al_2O_3 were not active for propane oxidation. However, this figure reveals NO conversion values at low temperatures probably due to NO oxidation on alumina surface or in the gas phase.

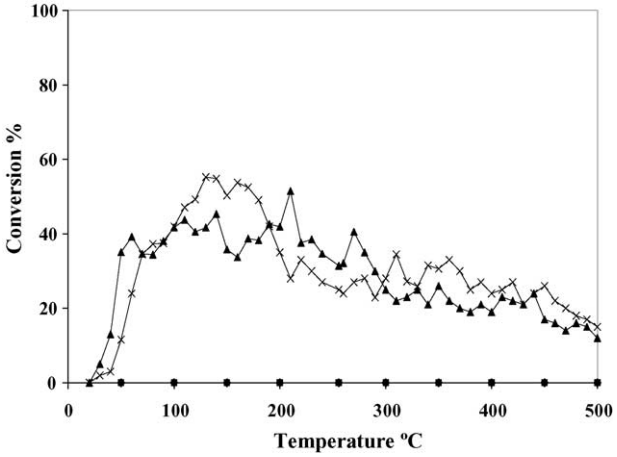

Fig. 1. Effect of temperature on the C_3H_8-NO-O_2 reaction over sulfated γ-Al_2O_3: (♦) C_3H_8, (×) NO; and unsulfated γ-Al_2O_3: (■) C_3H_8, (▲) NO. Feed, 1000 ppm of NO, 2.5 vol.% of C_3H_8, 15 vol.% of O_2, and balance He.

3.3. C_3H_8-NO-O_2 reactions over unsulfated Pt/γ-Al_2O_3 and unsulfated 1% Pt-2% Sn/γ-Al_2O_3 catalysts

The effect of temperature on the C_3H_8-NO-O_2 reaction over 1% Pt/γ-Al_2O_3 and 1% Pt-2% Sn/γ-Al_2O_3 unsulfated catalysts is shown in Fig. 2. In Fig. 3, temperatures of 50% conversion (light-off temperatures) are reported. In these figures, it can be seen that the temperature of 50% propane conversion is very similar for mono and bimetallic catalysts (259 and 262 °C, respectively). Thus, propane oxidation in not notably affected by the presence of tin in the catalyst.

The effect of temperature on NO% conversion during C_3H_8-NO-O_2 reaction is also shown in Fig. 2. NO% conversion as a function of temperature shows two peaks. The magnitude and position of the first peak remains unaffected on both 1% Pt/γ-Al_2O_3 and 1% Pt-2% Sn/γ-Al_2O_3 unsulfated catalysts. Over 1% Pt-2% Sn/γ-Al_2O_3 catalysts, the

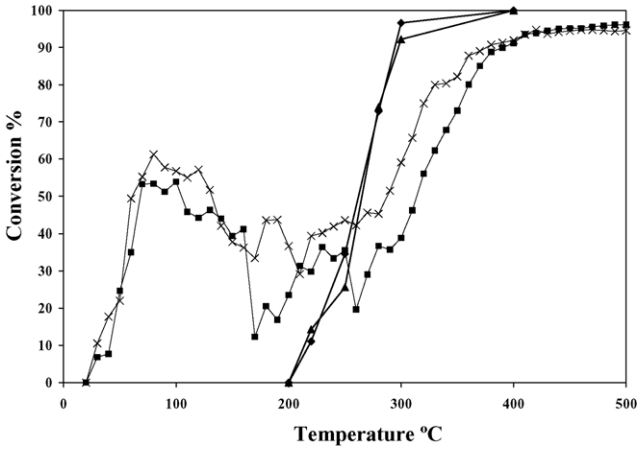

Fig. 2. Effect of temperature on the C_3H_8-NO-O_2 reaction over unsulfated 1% Pt /γ-Al_2O_3: (♦) C_3H_8, (■) NO; and unsulfated 1% Pt-2% Sn/γ-Al_2O_3: (▲) C_3H_8, (×) NO. Feed, 1000 ppm of NO, 2.5 vol.% of C_3H_8, 15 vol.% of O_2, and balance He.

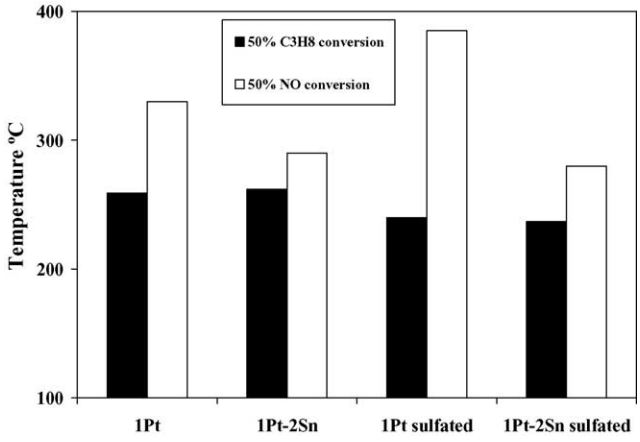

Fig. 3. Effect of sulfation of the 1% Pt/Al_2O_3 and 1% Pt-2% Sn/γ-Al_2O_3 catalysts on the temperatures of 50% conversion.

size of the second peak is slightly increased relative to 1% Pt/γ-Al_2O_3. In Fig. 3 it can be seen that the temperature of 50% NO conversion (second peak) is decreased over 1% Pt-2% Sn/γ-Al_2O_3 catalysts, relative to 1% Pt/γ-Al_2O_3 (290 and 330 °C, respectively).

In Fig. 4, total NO% conversion and % conversion to specific products (N_2, NO_2 and N_2O) at 100, 200, 300 and 400 °C is indicated. This figure reveals similar conversion values of N_2, NO_2 and N_2O for both catalysts. Thus, NO_x reactions are not notably affected by the presence of tin in the catalyst. However, a decrease of N_2O conversion at 300 °C is observed over 1% Pt-2% Sn/γ-Al_2O_3 relative to 1% Pt/γ-Al_2O_3.

3.4. C_3H_8-NO-O_2-SO_2 reactions over pre-sulfated 1% Pt/γ-Al_2O_3 and pre-sulfated 1% Pt-2% Sn/γ-Al_2O_3 catalysts

The evolution of C_3H_8-NO-O_2-SO_2 reactions over pre-sulfated 1% Pt/γ-Al_2O_3 and pre-sulfated 1% Pt-2% Sn/γ-Al_2O_3 catalysts is shown in Fig. 5. From the data in this figure and in Fig. 3, two major features emerge: (i) sulfating catalysts, results in a lowering of the 50% C_3H_8 conversion temperature on both catalysts. The shift in C_3H_8 light-off temperature on sulfation of Pt/γ-Al_2O_3 is well known [16]; and (ii) the temperature of 50% propane conversion is the same for mono and bimetallic pre-sulfated catalysts (240 and 237 °C, respectively).

The effect of temperature on NO% conversion during C_3H_8-NO-O_2-SO_2 reaction over pre-sulfated 1%Pt/γ-Al_2O_3 and pre-sulfated 1% Pt-2% Sn/γ-Al_2O_3 is also shown in Fig. 5. NO% conversion shows the same two peaks observed during C_3H_8-NO-O_2 reaction. A first observation is that the magnitude and position of the first peak remains unaffected on both pre-sulfated 1% Pt/γ-Al_2O_3 and pre-sulfated 1% Pt-2% Sn/γ-Al_2O_3. The second observation is that over pre-sulfated 1% Pt-2% Sn/γ-Al_2O_3 catalyst, the area of the second peak is increased relative to pre-sulfated 1% Pt/γ-Al_2O_3. Over pre-sulfated 1% Pt-2% Sn/γ-Al_2O_3, this peak

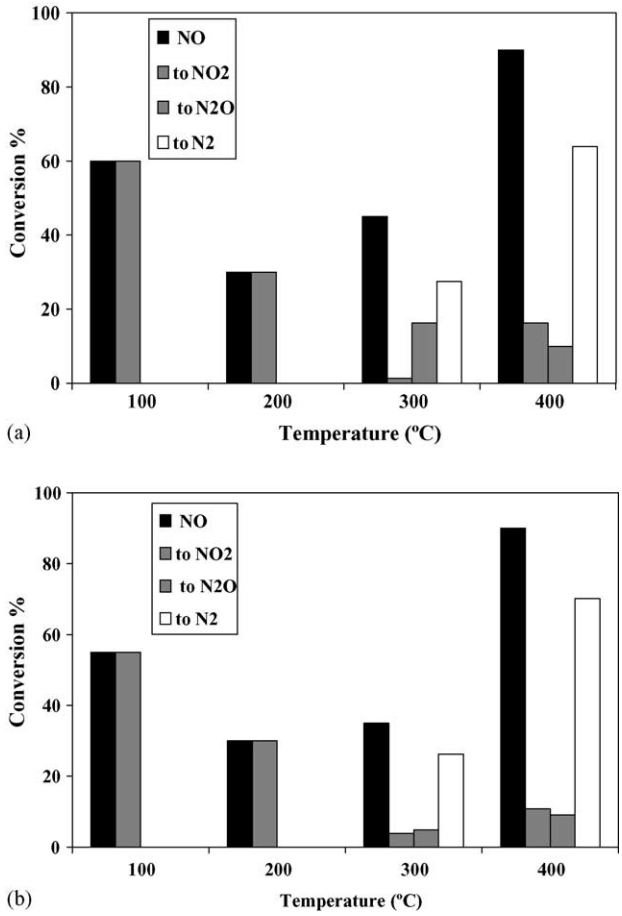

Fig. 4. Conversion of NO to NO_2, N_2O and N_2 measured at various temperatures. (a) Unsulfated 1% Pt/γ-Al_2O_3 and (b) unsulfated 1% Pt-2% Sn/γ-Al_2O_3.

arrives at its maximum value (90% conversion) at 350 °C. Over pre-sulfated 1% Pt/γ-Al_2O_3 the maximum value (66% conversion) arrives at 420 °C, showing a lower conversion value relative to the bimetallic catalyst. In Fig. 3, it can be seen

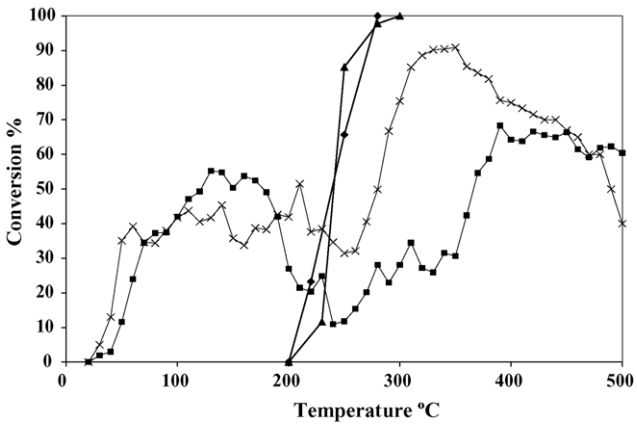

Fig. 5. Effect of temperature on the C_3H_8-NO-O_2-SO_2 reaction over pre-sulfated 1% Pt/γ-Al_2O_3: (♦) C_3H_8, (■) NO; and pre-sulfated 1% Pt-2% Sn/γ-Al_2O_3: (▲) C_3H_8, (×) NO. Feed, 1000 ppm of NO, 2.5 vol.% of C_3H_8, 50 ppm of SO_2, 15 vol.% of O_2, and balance He.

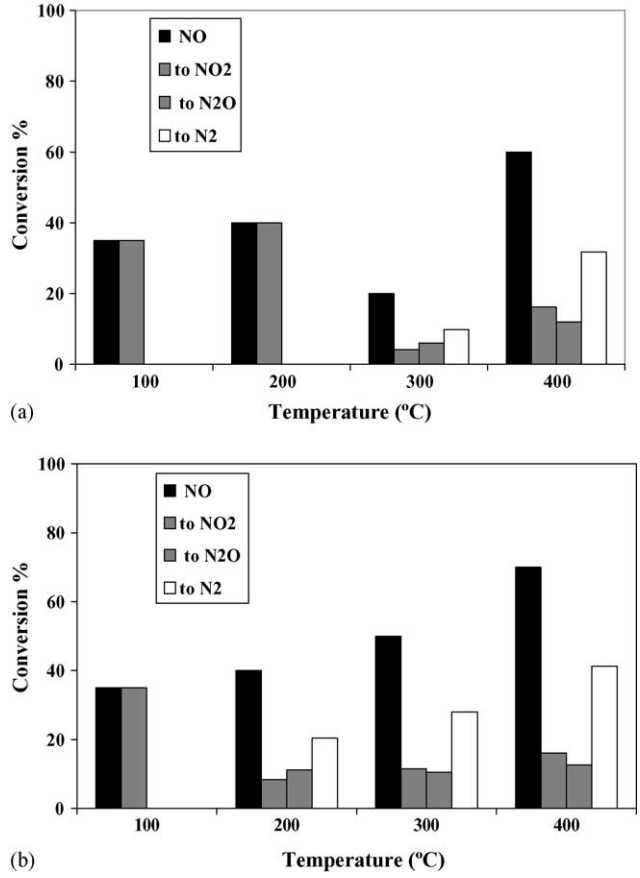

Fig. 6. Conversion of NO to NO_2, N_2O and N_2 measured at various temperatures. (a) Pre-sulfated 1% Pt/γ-Al_2O_3 and (b) pre-sulfated 1% Pt-2% Sn/γ-Al_2O_3.

that the temperature of 50% NO conversion (second peak) is strongly decreased over pre-sulfated 1% Pt-2% Sn/γ-Al_2O_3 catalysts, relative to pre-sulfated 1% Pt/γ-Al_2O_3 (280 and 385 °C, respectively).

Total NO% conversion and NO conversion to specific products (N_2, NO_2 and N_2O) at 100, 200, 300 and 400 °C over pre-sulfated catalysts are shown in Fig. 6. It is interesting to observe that: (i) N_2 production begins at 200 °C over pre-sulfated 1% Pt-2% Sn/γ-Al_2O_3 and only at 300 °C over pre-sulfated 1% Pt/γ-Al_2O_3; (ii) at the temperatures investigated, higher N_2% conversion is detected over pre-sulfated 1% Pt-2% Sn/γ-Al_2O_3 as compared with pre-sulfated 1% Pt/γ-Al_2O_3.

3.5. Quantitative analysis and localization of carbon residues

To investigate the effect of SO_2 present in the reaction feed on the resistance of catalysts to carbon residues deposition, a temperature-programmed oxidation on each catalyst was carried out after 12 h of C_3H_8 oxidation reaction. We studied carbon residues deposition on unsulfated 1% Pt/γ-Al_2O_3 and 1% Pt-2% Sn/γ-Al_2O_3 catalysts after 12 h of C_3H_8-NO-O_2 reaction (results shown in Fig. 7) and carbon residues

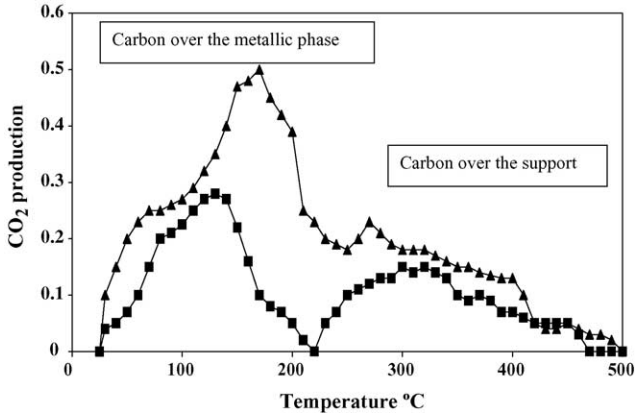

Fig. 7. TPO profile of carbon residues oxidation after 12 h of C_3H_8-NO-O_2 reaction over unsulfated 1% Pt/γ-Al_2O_3 (▲) and unsulfated 1% Pt-2% Sn/γ-Al_2O_3 (■).

deposition on pre-sulfated 1% Pt/γ-Al_2O_3 and pre-sulfated 1% Pt-2% Sn/γ-Al_2O_3 after 12 h of C_3H_8-NO-O_2-SO_2 reaction (results shown in Fig. 8). Now, it is well known, that in the case of reforming catalysts, temperature-programmed oxidation (TPO) shows two peaks that are particularly well resolved. The low temperature combustion (250–300 °C) corresponds to carbon residues deposited on the metallic phase, whereas the high temperature combustion is ascribed to carbon residues deposited on the support [18–20]. In these figures, it can be seen that sulfation of both 1% Pt/γ-Al_2O_3 and 1% Pt-2% Sn/γ-Al_2O_3 catalysts has a dramatic effect on the second (higher temperature) combustion signal. The effect of tin on carbon residues deposition is also seen in these figures. Tin addition to Pt/γ-Al_2O_3 lowers the amount of carbon deposited on the metallic phase (first peak). This effect is observed on pre-sulfated and unsulfated catalysts. It is worth noting that sulfation of 1% Pt-2% Sn/γ-Al_2O_3 results in a further diminution of the total amount of carbon residues deposited on the metallic phase.

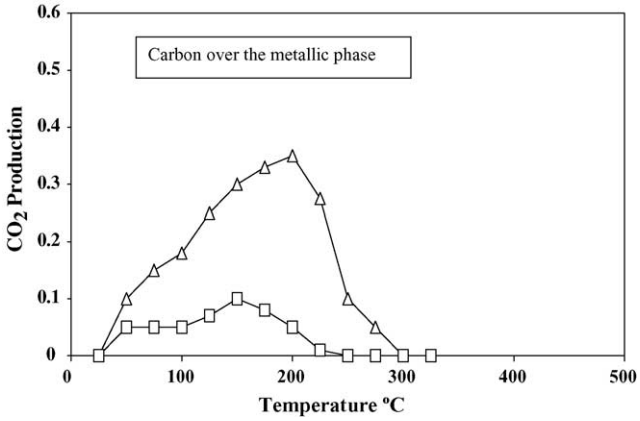

Fig. 8. TPO profile of carbon residues oxidation after 12 h of C_3H_8-NO-O_2 reaction over pre-sulfated 1% Pt/γ-Al_2O_3 (△) and pre-sulfated 1% Pt-2% Sn/γ-Al_2O_3 (□).

3.6. X-ray photoelectron spectroscopy

Binding energies of core electrons and surface atomic ratios of pre-sulfated and unsulfated catalysts are reported in Tables 2 and 3. The binding energy of Pt $4d_{5/2}$ for unsulfated 1% Pt/γ-Al_2O_3 (315.3 eV) indicates that Pt is present as Pt^0 [17]. A second Pt component is observed at higher binding energies (317.9 eV) corresponding to an oxidized species of Pt (Pt^{2+}) [17]. However, for the pre-sulfated 1% Pt/γ-Al_2O_3, 1% Pt-2% Sn/γ-Al_2O_3 (unsulfated and pre-sulfated) samples, the binding energy of Pt $4d_{5/2}$, revealed a higher binding energy component (318.4 eV) that can be associated to the presence of Pt in a higher oxidation state (Pt^{4+}) [18–23]. For the catalysts with Sn, the binding energy of Sn $3d_{5/2}$ (close to 487 eV) reveals that Sn is present as Sn^{2+} [17,24,25]. The binding energy of Sn $3d_{5/2}$ for pre-sulfated 1% Pt-2% Sn/γ-Al_2O_3, presents a second component (484 eV) that can be associated with traces of a reduced phase (as Sn^0 or one alloyed phase $SnPt_x$). For the sulfated samples, the binding energy of the S $2p_{3/2}$ (168.9 eV) revealed that S is only present as S^{6+} [26,27], thus only sulfate species are present in the catalyst.

It is worth noting in Table 3, that the Pt/Al XPS signal ratio increases substantially with Sn addition (0.0020 for 1% Pt/γ-Al_2O_3 and 0.0053 for 1% Pt-2% Sn/γ-Al_2O_3). This increase cannot be due to an increase in Pt dispersion since Sn addition lowers Pt dispersion, but to Sn spreading on and masking the alumina (i.e. Sn spreads on the alumina support on the vicinity of Pt particles). This explanation can account also for the increase of the S/Al XPS signal ratio of pre-sulfated 1% Pt-2% Sn/γ-Al_2O_3 (0.099) relative to pre-sulfated 1% Pt/γ-Al_2O_3 (0.081). The increase cannot be due to an increase in sulfate formation as Sn addition lowers SO_2 oxidation (Table 3). It is likely that Sn masks the alumina.

Table 2
Binding energies (eV) of core electrons of alumina-supported Pt-Sn catalysts

Catalyst	Sn $3d_{5/2}$	Pt $4d_{5/2}$	S 2p
1% Pt/γ-Al_2O_3	–	315.3 (56) 317.9 (44)	
1% Pt/γ-Al_2O_3 pre-sulfated	–	315.4 (51) 318.4 (49)	168.9
1% Pt-2% Sn/γ-Al_2O_3	486.8	315.8 (60) 318.3 (40)	
1% Pt-2% Sn/γ-Al_2O_3 pre-sulfated	484.0 (6) 486.9 (94)	315.2 (67) 318.3 (33)	169.0

In parenthesis are peak percentages.

Table 3
Atomic surface ratios of supported Pt and Pt-Sn catalysts determined by XPS

Catalyst	S/Al	Sn/Al	Pt/Al
1% Pt/γ-Al_2O_3	0.0	0.0	0.0020
1% Pt/γ-Al_2O_3 pre-sulfated	0.081	0.0	0.0014
1% Pt-2% Sn/γ-Al_2O_3	0.0	0.043	0.0053
1% Pt-2% Sn/γ-Al_2O_3 pre-sulfated	0.099	0.0374	0.0050

4. Discussion

The 1% Pt/γ-Al_2O_3 catalyst was pre-sulfated under oxidizing conditions, which is expected to result in the formation of sulfate species on the Al_2O_3 support, but does not result in any sulfur species being deposited on Pt [28,29].

The C_3H_8 oxidation is unaffected by Sn present in the 1% Pt/γ-Al_2O_3 catalyst, which is then consistent with the mechanism proposing that the reaction occurs only on the Pt surface. However, pre-sulfation of the 1% Pt/γ-Al_2O_3 catalyst results in lowering of the C_3H_8 light-off temperature (Fig. 3). Moreover, the shift in C_3H_8 light-off temperature on sulfation of the 1% Pt/γ-Al_2O_3 catalyst results unaffected by the presence of SO_2 in the reaction feed. Over 1% Pt-2% Sn/γ-Al_2O_3, sulfation also results in a shift in C_3H_8 light-off temperature even in the presence of SO_2 in the reaction feed. In Fig. 3, it is worth noting the similarity of the shift in C_3H_8 light-off on sulfation of 1% Pt/γ-Al_2O_3 and 1% Pt-2% Sn/γ-Al_2O_3 catalysts.

It is well known that selective reduction of NO with hydrocarbons is a very complex reaction comprising several parallel or consecutive reaction steps. It has been proposed a reaction mechanism of NO reduction by propane over Pt/Al_2O_3 [30]. NO reduction appears to occur via reaction of NO_2 with C_3H_8 on the support and/or at the metal-support interface. Sulfation of the Al_2O_3 results in a decrease in the number of sites available for the nitrate species to be adsorbed and hence in the number of adsorbed nitrate species with which propane or propane derivate species can react, according to the following mechanism:

$$NO + O_2 \rightarrow NO_2 \rightarrow NO_3^- (ads) \quad (1)$$

$$C_3H_8 + O_2 \rightarrow [C_xH_yO_z] \rightarrow CO_x + H_2O \quad (2)$$

$$NO_3^- (ads) + [C_xH_yO_z] \rightarrow N_2\,CO_x + H_2O \quad (3)$$

The inhibition effect of sulfation on the catalytic activity for NO reduction by hydrocarbons has been reported for many alumina-based catalysts [30–32].

In Figs. 2, 3 and 5, the inhibition effect of sulfation on NO% conversion over sulfated 1% Pt/γ-Al_2O_3 is observed. In Fig. 3 it can be seen that pre-sulfation of the 1% Pt/γ-Al_2O_3 catalyst results in increasing the NO light-off temperature (330 and 385 °C for unsulfated 1% Pt/γ-Al_2O_3 and pre-sulfated 1% Pt /γ-Al_2O_3, respectively).

This negative effect of sulfation on NO% conversion over pre-sulfated 1% Pt/γ-Al_2O_3 is probably due to (i) the strong adsorption of sulfates on the alumina sites at which NO_2 adsorption occurs; and (ii) the sintering of Pt during the sulfation process. The last assumption is supported by the decrease of the Pt/Al ratio with sulfation (Table 3) of the 1% Pt/γ-Al_2O_3 catalyst determined by XPS (0.0020 for unsulfated 1% Pt/γ-Al_2O_3 and 0.0014 for pre-sulfated 1% Pt/γ-Al_2O_3). Sintering of Pt particles may lead to a diminution of the available Pt surface sites at which NO oxidation occurs, thus lowering NO conversion as shown in Fig. 4. This result could be

confirmed following the NO_2 generation during the process. NO_2 production might be higher over unsulfated 1% Pt/γ-Al_2O_3 relative to pre-sulfated 1% Pt/γ-Al_2O_3. However, NO_2 determination during the process is meaningless since reaction (1) shows that NO_2 generated by NO oxidation, reacts consecutively with oxygen present forming NO_3^-.

Sulfation of 1% Pt-2% Sn/γ-Al_2O_3 catalyst should also result in a negative effect on NO% conversion due to:

(i) The strong adsorption of sulfates on the alumina sites at which NO_2 adsorption occurs. However, in a recent work [10], we showed that during the sulfation process, tin addition to 1% Pt/γ-Al_2O_3 resulted in lowering the SO_2 interactions with oxygen leading to a diminution of sulfates generated over the surface of the catalyst (Table 1), consequently, in an increase in the number of sites available on alumina for nitrate species to be adsorbed during C_3H_8-NO-O_2-SO_2 reactions.

(ii) The sintering of Pt during the sulfation process. However, in Table 3, it can be seen that the values of Pt/Al atomic surface ratios determined by XPS are 0.0053 and 0.0050 over unsulfated 1% Pt-2% Sn/γ-Al_2O_3 and over pre-sulfated 1% Pt-2% Sn/γ-Al_2O_3, respectively. These results show that Pt surface remains unchanged during sulfation, suggesting that tin addition to a 1% Pt/γ-Al_2O_3 catalyst, prevents Pt particles from sintering during this process. The prevention of Pt particles sintering by Sn addition and the diminution of sulfates generated over the surface of the catalyst explain the fact, that in our conditions, pre-sulfated 1% Pt-2% Sn/γ-Al_2O_3 is more active than pre-sulfated 1% Pt/γ-Al_2O_3 for NO conversion according to reaction (1). This assumption is supported by the results obtained in this work, shown in Figs. 2 and 5. It is interesting to note in Figs. 3 and 5 that during C_3H_8-NO-O_2-SO_2 reactions, higher % N_2 generation is observed over pre-sulfated 1% Pt-2% Sn/γ-Al_2O_3 relative to pre-sulfated 1% Pt/γ-Al_2O_3.

4.1. Carbon residues deposition

The distinction between carbon deposited on the metallic surface and on the support can be performed by the thermo-programmed oxidation of a catalyst [33]. From results shown in Figs. 7 and 8, two major features emerge:

(i) Sulfation of 1% Pt/γ-Al_2O_3 and 1% Pt-2% Sn/γ-Al_2O_3 catalysts, results in a complete inhibition of deposition of carbon residues on the support after the C_3H_8-NO-O_2-SO_2 reaction. Sulfate species formed over the support during sulfation may result in a strong decrease in the number of sites available on the alumina for carbon residues species to be adsorbed.
The lower deposition of carbon residues on the metallic surface of sulfated 1% Pt/γ-Al_2O_3 related to non-sulfated 1% Pt/γ-Al_2O_3 can be explained on basis of XPS results compiled in Table 3. Pt/Al atomic surface ratio of unsulfated 1% Pt/γ-Al_2O_3 is higher related to pre-sulfated 1% Pt/γ-Al_2O_3 (0.0020 and 0.0014, respectively). Thus the lower Pt surface present in the sulfated catalyst may generate lower amounts of carbon residues deposition on the metallic surface.

(ii) Tin addition to 1% Pt/γ-Al_2O_3 results in a diminution of carbon deposited on the metallic phase. This diminution can be explained on basis of the early studies of Lieske et al. [34] who showed that addition of tin to platinum gave coke precursors that were more mobile and could migrate more easily to the alumina, thus, resulting in a larger part of Pt remaining free. Now, in Figs. 7 and 8 it can be observed that pre-sulfated 1% Pt-2% Sn/γ-Al_2O_3 catalyst leads to a further diminution of carbon deposited on the metallic phase related to unsulfated 1% Pt-2% Sn/γ-Al_2O_3. This result can also be explained on basis of XPS determinations. Results presented in Table 3 show the binding energies of core electrons of pre-sulfated and unsulfated 1% Pt-2% Sn/γ-Al_2O_3 catalysts. For Sn containing catalysts, the binding energy Sn $3d_{5/2}$ (close to 487 eV) reveals that Sn is present as Sn^{2+}. The binding energy Sn $3d_{5/2}$ for sulfated 1% Pt-2% Sn/γ-Al_2O_3 presents a second component (483.9 eV) that can be associated with a reduced phase (as Sn^0 or one alloyed phase $SnPt_x$), that may induce a higher dilution of Pt surface ensembles resulting in an additional lowering of carbon deposits precursors.

5. Conclusions

Two main conclusions are derived from the study of the (SCR) of NO with C_3H_8 over unsulfated and pre-sulfated 1% Pt /γ-Al_2O_3, and 1% Pt-2% Sn/γ-Al_2O_3 catalysts: (i) tin addition to 1% Pt/γ-Al_2O_3 results in a diminution of sulfates generated during sulfation over the surface of the catalyst thus in an increase in the number of sites available on alumina for nitrate species to be adsorbed during C_3H_8-NO-O_2-SO_2 reactions; (ii) tin addition to a 1% Pt/γ-Al_2O_3 catalyst, prevents Pt particles from sintering during sulfation process thus Pt surface remains unchanged for NO oxidation. These facts are probable factors responsible of the high resistance of pre-sulfated 1% Pt-2% Sn/γ-Al_2O_3 on the deactivation by sulfur of NO conversion.

We also investigated the effect of Sn addition to 1% Pt/γ-Al_2O_3 catalyst, and the effect of pre-sulfation on 1% Pt/γ-Al_2O_3 and 1% Pt-2% Sn/γ-Al_2O_3, on carbon depositions over the catalysts. The lower activity in carbon deposition over the metallic surface of 1% Pt-2% Sn/γ-Al_2O_3, relative to 1% Pt/γ-Al_2O_3, can be explained in basis of the presence of Sn species that may induce a dilution of Pt surface ensembles lowering carbon deposits precursors. The lowering on carbon deposition on the support on both sulfated 1% Pt/γ-Al_2O_3 and 1% Pt-2% Sn/γ-Al_2O_3 can be explained on basis of sulfate species formed over the support during sulfation that may result in a strong decrease in the number of sites available on the alumina for carbon residues species to be adsorbed.

The facts that tin addition to a Pt/γ-Al_2O_3 catalyst prevents Pt particles from sintering during high temperature sulfation process and that sulfating a Pt-Sn/γ-Al_2O_3 catalyst prevents carbon residues deposition over the catalyst, suggest that pre-sulfated 1% Pt-2% Sn/γ-Al_2O_3 catalyst may prevent further contributions to particulate formation over the catalyst and increase catalyst resistance to deactivation during automotive exhaust control.

References

[1] The Impact of Sulfur in Diesel Fuel on Catalyst Emission Control Technology, MECA, http://www.meca.org, 1999.
[2] V.I. Parvulescu, P. Grange, B. Delmon, Catal. Today 46 (1998) 233.
[3] E.A. Efthimiadis, G.D. Lionta, S.C. Chrisoforou, I.A. Vasalos, Catal. Today 40 (1998) 15.
[4] H.Y. Huang, R.Q. Long, R.T. Yang, Appl. Catal. B 33 (2001) 127.
[5] F.C. Meunier, J.R.H. Ross, Appl. Catal. B 24 (2000) 23.
[6] A. Obuchi, A. Ohi, M. Nakamura, A. Ogata, K. Mizuno, H. Obuchi, Appl. Catal. B 2 (1993) 71.
[7] G. Zhamg, T. Yamaguchi, H. Kawakami, T. Suzuki, Appl. Catal. B 1 (1992) L15.
[8] K.M. Adams, J.V. Cavataio, R.H. Hammerle, Appl. Catal. B 10 (1996) 157.
[9] R. Burch, T.C. Walting, Appl. Catal. B 17 (1998) 131.
[10] G. Corro, R. Montiel, J. Mol. Catal. A 184 (2002) 443.
[11] H. Lieske, J. Volter, J. Catal. 25 (1984) 96.
[12] K. Balakirshnan, J. Schwank, J. Catal. 127 (1991) 287.
[13] R.D. Cortright, J.A. Dumesnic, J. Catal. 157 (1995) 576.
[14] G.T. Baronetti, S.R. De Miguel, O.A. Scelza, M.A. Fritzer, A.A. Castro, Appl. Catal. 19 (1985) 77.
[15] J. Volter, G. Lietz, M. Uhlemann, M. Hermann, J. Catal. 68 (1981) 42.
[16] H.C. Yao, H.K. Stepien, H.S. Gandhi, J. Catal. 67 (1981) 231.
[17] D. Briggs, M.P. Seah (Eds.), Practical Surface Analysis by Auger and X-ray Photoelectron Spectroscopy, second ed., Wiley, Chichester, UK, 1990.
[18] J. Escard, B. Pontvianne, M.T. Chenebaux, J. Cosyns, Bull. Soc. Chem. Fr. 11 (1975) 2399.
[19] E. Czaran, J. Finster, K.H. Schnabel, Z. Anorg. Allg. Chem. 443 (1978) 175.
[20] Z. Zsoldos, L. Guczi, J. Phys. Chem. 96 (1992) 23.
[21] L. Guczi, A. Sarkany, Z. Koppany, Appl. Catal. 120 (1994) L1.
[22] V.R. Choudhary, V.H. Rane, J. Catal. 130 (1991) 411.
[23] G. Corro, J.L.G. Fierro, O. Vazquez, Catal. Commun. 4 (2003) 371.
[24] J. Llorca, N. Homs, J. Leon, J. Sales, J.L.G. Fierro, P. Ramirez de la Picina, Appl. Catal. A 189 (1999) 77.
[25] C.L. Lau, G.K. Wertheim, J. Vac. Sci. Technol. 15 (1978) 622.
[26] U. Kohler, H.W. Wassmuth, Surf. Sci. 122 (1982) 491.
[27] R.C. Ku, P. Wynblatt, Appl. Surf. Sci. 8 (1981) 250.
[28] D.D. Beck, M.H. Krueger, D.R. Monroe, SAE Technical Paper 910844 (1991).
[29] C.R. Apesteguia, T.G. Garetto, A. Borgna, J. Catal. 106 (1987) 73.
[30] R. Burch, J.A. Sullivan, T.C. Walting, Catal. Today 42 (1998) 13.
[31] M. Tabata, H. Tsuchida, k. Miyamoto, T. Yoshinari, H. Yamasaki, H. Hamada, Y. Kintaichi, M. Sasaki, T. Ito, Appl. Catal. B 6 (1995) 169.
[32] K. Kung, P.W. Park, D.W. Kim, H.H. Kung, J. Catal. 181 (1999) 1.
[33] J. Barbier, G. Corro, Y. Zhang, J.P. Bournonville, J.P. Frank, Appl. Catal. 13 (1985) 245.
[34] H. Lieske, J. Volter, J. Catal. 25 (1984) 96.